Proceedings of the ASME 2021
International Design Engineering Technical Conferences
& Computers and Information in Engineering Conference
IDETC/CIE 2021
August 17-20, 2021, Online, Virtual, USA

# IDETC2021-70067

# High-Dimensional Reliability Method Accounting for Important and Unimportant Input Variables

Jianhua Yin<sup>1, 2</sup>, Xiaoping Du<sup>1, \*</sup>

<sup>1</sup>Department of Mechanical and Energy Engineering, Indiana University - Purdue University Indianapolis, IN, United States

<sup>2</sup>School of Mechanical Engineering, Purdue University, West Lafayette, IN, United States

#### **Abstract**

Reliability analysis is usually a core element in engineering design, during which reliability is predicted with physical models (limit-state functions). Reliability analysis becomes computationally expensive when the dimensionality of input random variables is high. This work develops a high dimensional reliability analysis method by a new dimension reduction strategy so that the contributions of both important and unimportant input variables are accommodated by the proposed dimension reduction method. The consideration of the contributions of unimportant input variables can certainly improve the accuracy of the reliability prediction, especially where many unimportant input variables are involved. The dimension reduction is performed with the first iteration of the first order reliability method (FORM), which identifies important and unimportant input variables. Then a higher order reliability analysis, such as the second order reliability analysis and metamodeling method, is performed in the reduced space of only important input variables. The reliability obtained in the reduced space is then integrated with the contributions of unimportant input variables, resulting in the final reliability prediction that accounts for both types of input variables. Consequently, the new reliability method is more accurate than the traditional method, which fixes unimportant input variables at their means. The accuracy is demonstrated by three examples.

Keywords: reliability analysis; dimension reduction; physics-based reliability

## 1. Introduction

In engineering design, physics-based reliability is commonly used to predict the probability of failure using physical models derived from physical principles. Such a model is called a limit-state function and is given by

$$Y = g(\mathbf{X}) \tag{1}$$

where  $\mathbf{X}$  is a vector to represent random input variables, and  $\mathbf{Y}$  is a response that indicates the occurrence of a failure.

Physics-based reliability methods can be divided into three categories: numerical methods [1-5], surrogate methods [6-13], and simulation methods [14-16]. Typically, numerical methods simplify the limit-state function (Eq. 1) using the first or second order Taylor expansion, and the reliability approximated by the simplified function. The surrogate methods construct an easyaccess model utilizing sensitivity analysis, Design of Experiments (DoE), and active learning methods, etc., and the reliability obtained by evaluating the surrogate model instead of the original limit-state function. However, both numerical and surrogate methods suffer from the curse of dimensionality that makes reliability analysis computationally expensive for highdimensional problems. Because reliability prediction repeatedly calls limit-state functions, which are typically complex, resource-intensive numerical models. The number of function call grows drastically as the increase of dimensionality of the input variables. Although the efficiency of simulation methods, such as Monte Carlo Simulation (MCS) [17] and importance sampling method [18], is not affected by the dimensionality, they

© 2021 by ASME

<sup>\* 723</sup> W. Michigan Street, Indianapolis, IN 46202-5195, USA, Email: duxi@iu.edu

are still computationally expensive when the reliability is high and may not be practically used in engineering design.

High-dimensional reliability analysis is encountered in many engineering and science fields [19-23]. Current highdimensional analysis methods are roughly classified into three types. The first type includes methods [24-27] using highdimensional model representation (HDMR), which decomposes a high dimensional limit-state function g(X) into the sum of several lower-dimensional functions. The moments (means, variance, etc.) of the response can be approximated by several low dimensional numerical integrations. However, the accuracy of the reliability obtained by HDMR may not accurate enough if the interaction terms are dominant. The low dimensional functions are usually approximated by Taylor expansion, which also introduces errors. Although the accuracy of the reliability assessment can be improved by increasing the approximation order, the number of function evaluations may increase drastically. Balancing the prediction accuracy and efficiency remains challenging for HDMR.

The second type of method [28-35] combines dimension reduction with surrogate modeling and machine learning. Three steps are usually involved. Step 1 is the dimension reduction performed by sliced inverse regression (SIR) [29, 32, 36] or other methods [24, 31] at specific training points, usually generated through DoE [37]. Important input variables are identified. In Step 2 a surrogate model is constructed with respect to important input variables in the reduced dimensional space. Many regression and machine learning methods could be used for this purpose, including Polynomial Chaos Expansion [29], Gaussian Process Regression [38], Support Vector Machines [39], and Neural Network [30]. Step 3 is the surrogate model validation. After the accuracy of the surrogate model is validated, it is used to estimate the reliability, and MCS is usually used. A sufficient number of training points are needed for the good accuracy of the surrogate model. The number of training points, thereby the number of function calls, increases greatly with the increase of dimensionality of input variables.

The third most commonly used method is principal component analysis (PCA) [40-42]. PCA reduces the dimension of the input variables by making use of the correlations between the input variables. Therefore, PCA works well for the elements of input variables that are strongly correlated. When the input variables are independent or only weakly correlated, PCA may not work well for dimension reduction. Besides, PCA does not use the information of the response Y, and it is, therefore, an unsupervised dimension reduction technique. Although dimension reduction is optimal in the given data space, it may be suboptimal for the entire regression space.

Overall, despite the progress, numerous challenges remain in the path toward routinely accommodating high dimensional problems in reliability analysis. In most of the successful applications, only dozens of random input variables can be practically handled except the special cases involving functional data [28, 29]. However, the dimension of input variables could easily add up to hundreds or thousands in system design. For example, the aircraft wing optimization design [43, 44] involves

structure and aerodynamics. The numbers of design variables, random variables, and constraints could be in hundreds or thousands. Moreover, when the reliability requirement is high, accurately predicting the reliability is extremely computation demand.

In real engineering applications, not all the elements of  $\mathbf{X}$  contribute significantly to the response  $\mathbf{Y}$ . The majority elements of  $\mathbf{X}$  may have insignificant effects that are, therefore, unimportant variables. Their total effect, however, may not negligible because the unimportant variables may count for most of  $\mathbf{X}$ . Traditional dimension reduction methods usually neglect the contribution of the unimportant variables because they are fixed at their means, and this can lead to a large error.

In this study, we account for the total effect of unimportant variables by fixing them at their percentiles so that the dimension is reduced but the influence of unimportant variables is not neglected. The proposed method does not require random sampling for dimension reduction. Instead, it is based on a numerical method, or the First Order Reliability Method (FORM). After dimension reduction, any reliability method with higher accuracy can be used to predict the reliability since the computational effort will be reduced significantly in the reduced space. Then the predicted reliability is combined with the contribution of the unimportant variables to produce the final reliability prediction.

The remainder of this paper is organized as follows. Section 2 reviews the methodologies that this study uses. Section 3 discusses the details of the proposed method, followed by three examples in Section 4. The conclusions are provided in Section 5.

## 2. Review

In this section, we briefly review the basic knowledge that is related to the proposed method, FORM, the Second Order Reliability Method (SORM), and the Second Order Saddlepoint Approximation (SOSPA). The rules of symbols in this paper are: 1) a capitalized letter in bold denotes a vector of random variables (e.g.,  $\mathbf{X}$  or  $\mathbf{U}$ ), 2) a lower-case letter in bold denotes a vector of deterministic variables (e.g.,  $\mathbf{X}$  or  $\mathbf{u}$ ), 3) an italicized capital letter denotes a random variable (e.g.,  $\mathbf{X}$  or  $\mathbf{U}$ ), and 4) an italicized lowercase letter of denotes a deterministic variable (e.g.,  $\mathbf{X}$  or  $\mathbf{u}$ ).

## 2.1 FORM and SORM

The reliability is defined by the following probability

$$R = \Pr\{g(\mathbf{X}) \ge 0\} \tag{2}$$

The probability of failure  $p_f$  is then given by

$$p_f = 1 - R = \Pr\{g(\mathbf{X}) < 0\} = \int_{g(\mathbf{X}) < 0} f_{\mathbf{X}}(\mathbf{x}) < 0 \, d\mathbf{x}$$
 (3)

where  $f_{\mathbf{X}}(\mathbf{x})$  is the joint probability density function (PDF) of **X**. The limit-state function  $g(\mathbf{X})$  is usually a nonlinear function. In this study, we assume all the elements in **X** are independent. Directly integrating the PDF in the region of  $g(\mathbf{X}) < 0$  is often

impractical and computationally expensive. It is the reason that many approximation methods have been developed, including FORM [1] and SORM [3], where three steps are involved.

1) Transform **X** into the standard normal variables **U** by

$$F_{X_i}(X_i) = \Phi(U_i) \tag{4}$$

where  $F_{X_i}(\cdot)$  and  $\Phi(\cdot)$  represent the cumulative density function (CDF) of  $X_i$  and  $U_i$ , respectively. Denote the transformation by  $\mathbf{X} = T(\mathbf{U})$ , and Eq. (3) is rewritten as

$$\Pr\{g(\mathbf{X}) < 0\} = \int_{g(T(\mathbf{U})) < 0} f_{\mathbf{U}}(T(\mathbf{u})) < 0 \ d\mathbf{u}$$
 (5)

where  $f_{\mathbf{U}}(\cdot)$  is the joint PDF of **U**.

2) Find the most probable point (MPP) which is a point with the highest PDF on the surface of  $g(\mathbf{U}) = 0$ . Geometrically, MPP has the shortest distance from the surface to the origin in U-space, and then MPP  $\mathbf{u}^*$  is found by

$$\begin{cases}
\min_{\mathbf{u}} \beta = \|\mathbf{u}\| \\
\text{subject to } g(\mathbf{U}) = 0
\end{cases}$$
(6)

where  $\|\cdot\|$  stands for the length of a vector.  $\beta = \|\mathbf{u}^*\|$  is the reliability index because it is related to the probability of failure as will be shown in Eq. (9).

3) Approximate the limit-state function linearly (FORM) or quadratically (SORM) at u\*. The use of u\* can minimize the error of the approximation. The two approximations are given by

$$g(\mathbf{U}) \approx g(\mathbf{u}^*) + \nabla g(\mathbf{u}^*)^{\mathrm{T}} (\mathbf{U} - \mathbf{u}^*)$$
 (7)

$$g(\mathbf{U}) \approx g(\mathbf{u}^*) + \nabla g(\mathbf{u}^*)^{\mathrm{T}} (\mathbf{U} - \mathbf{u}^*) + \frac{1}{2} (\mathbf{U} - \mathbf{u}^*)^{\mathrm{T}} H(\mathbf{u}^*) (\mathbf{U} - \mathbf{u}^*)$$
(8)

where  $\nabla g(\mathbf{u}^*)$  and  $H(\mathbf{u}^*)$  are the gradient and the Hessian matrix of  $g(T(\mathbf{U}))$  with respect to  $\mathbf{u}^*$ , respectively.

After the three steps, FORM gives

$$p_f = \Phi(-\beta) \tag{9}$$

As mentioned previously,  $\beta$  is called the reliability index, and when FORM is used,  $\beta$  is also the magnitude of the MPP as indicated in Eq. (6). For this reason, we call  $\beta$  from FORM the FORM-reliability index throughout the paper. The solution from SORM is in general more accurate and is obtained by multiplying Eq. (9) with a correction term [3].

## 2.2 SOSPA

SOSPA [45] is also a second-order approximation method based on SORM and saddlepoint approximation (SPA) [46, 47]. SOSPA uses the cumulant generating function (CGF)  $K_Y(t)$ , which can be derived analytically from the approximated

response in Eq. (8). Once  $K_Y(t)$  is available, the saddlepoint  $t_S$  is obtained by solving

$$K_Y'(t) = 0 (10)$$

where  $K'_g(t)$  is the first derivative of the CGF. Then,  $p_f$  is computed by [48]

$$p_f = \Phi(\omega) + \phi(\omega) \left(\frac{1}{\omega} - \frac{1}{\nu}\right) \tag{11}$$

where  $\phi(\cdot)$  represents the PDF of the standard normal distribution.

$$\omega = \operatorname{sgn}(t_s) \{ 2[-K_Y(t_s)] \}^{\frac{1}{2}}$$
 (12)

$$\nu = t_s [K_Y''(t_s)]^{\frac{1}{2}}$$
 (13)

where  $sgn(\cdot)$  is the signum function, which equals to 1, -1, or 0 when  $t_s$  is positive, negative or zero, respectively;  $K_a''(t_s)$  is the second derivative of the CGF with respect to t.

# 3. Methodology

The distinctive strategy of the proposed method is to use an accurate reliability method in the reduced space and also account for the contributions of both important and unimportant input variables to the reliability.

#### 3.1 Overview

The purpose of dimension reduction is to identify important and unimportant variables in X. We will use FORM to perform the dimension reduction since the MPP from FORM can directly measure the importance of input variables for two reasons. First, the reliability is determined by the FORM-reliability index or the magnitude of the MPP since  $\beta = \|\mathbf{u}^*\| = \sqrt{\sum_{i=1}^n (u_i^*)^2}$ ; second, the components of the MPP  $\mathbf{u}^* = (u_i^*)_{i=1,n}$  determine the importance of the elements of X or their contributions to the reliability. As shown in Fig. 1, a farther distance from the mean (or median) means a larger value of the MPP component and, therefore, a higher contribution. Hence, we can use the MPP components to identify both important and unimportant input variables. Since the MPP components of the unimportant input variables do not change significantly during the MPP search, we propose to use the MPP obtained from the first iteration of the MPP search, and this can greatly reduce the computational effort.

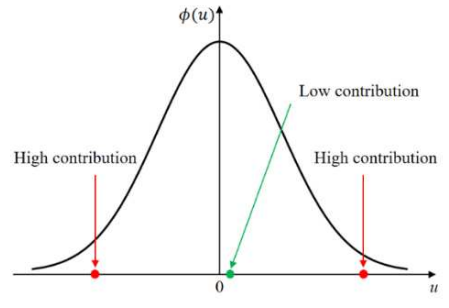


Fig. 1 Percentile of a random variable

Once the MPP is obtained from the first iteration, important and unimportant input variables are identified by their MPP components. Then the subsequent analysis will be conducted with only important variables, and a reliability method with higher accuracy can be used with the unimportant input variables fixed at their MPP components. Using a high accurate reliability method is affordable because the number of function calls can be reduced in the reduced space. Then the final reliability is obtained by integrating the reliability obtained in the reduced space and the FORM-reliability index of unimportant input variables.

The proposed method involves three steps: 1) dimension reduction, 2) reliability analysis in the reduced space, and 3) reliability analysis in the original space.

#### 3.2 Dimension reduction

The purpose of the first step is to identify important and unimportant input variables. This step involves the first iteration of the MPP search and starts from the origin of the U-space. Set the initial point at the origin  $\mathbf{u}_0 = (0,0,...,0)^T$  and calculate the initial FORM-reliability index  $\beta_0 = ||\mathbf{u}_0|| = 0$ . We obtain the gradient at  $\nabla g(\mathbf{u}_0)$  and approximate the limit-state function by

$$g(\mathbf{U}) \approx g(\mathbf{u}_0) + \nabla g(\mathbf{u}_0)^{\mathrm{T}} \mathbf{U}$$
 (14)

The unit vector  $\boldsymbol{\alpha}$  of  $\nabla g(\mathbf{U})$  at  $\mathbf{u}_0$  is given by

$$\alpha = \frac{\nabla g(\mathbf{u}_0)}{\|\nabla g(\mathbf{u}_0)\|} \tag{15}$$

Then the FORM-reliability index of one-step MPP is obtained by

$$\beta_1 = \beta_0 + \frac{g(\mathbf{u}_0)}{\|\nabla g(\mathbf{u}_0)\|} = \frac{g(\mathbf{u}_0)}{\|\nabla g(\mathbf{u}_0)\|}$$
(16)

Using the fact that the MPP vector is in the opposite direction of the gradient [49], we have the first iteration of the MPP  $\mathbf{u}_1$ .

$$\mathbf{u}_1 = -\beta_1 \mathbf{\alpha} = -\frac{g(\mathbf{u}_0) \nabla g(\mathbf{u}_0)}{\|\nabla g(\mathbf{u}_0)\|^2}$$
(17)

And it can be easily approved that  $\beta_1 = ||\mathbf{u}_1||$  holds for Eqs. (16) and (17).

As discussed previously, the magnitude of each component in the MPP vector indicates the importance of the input variable. We then set up a threshold c to distinguish important input variables from unimportant ones. If  $u_{1i} \leq c$ ,  $U_i$  is considered an unimportant variable; otherwise,  $U_i$  is considered an important variable. There are several ways to determine c. For instance, we can set c=0.1, which means 0.1 standard deviations from the mean, below which the variable is thought to be unimportant. Or we can use c=1%, 2%, or 3%  $\beta_1$ .

We group the important variables into a vector  $\overline{\bf U}$  and group the unimportant variables into a vector  $\underline{\bf U}$  with the dimensions of  $\overline{n}$  and  $\underline{n}$ , respectively. Then the input variables are partitioned into two parts.

$$\mathbf{U} = \left(\overline{\mathbf{U}}; \ \underline{\mathbf{U}}\right) \tag{18}$$

Accordingly, the first-iteration MPP is also partitioned into two parts.

$$\mathbf{u}_1 = \left(\overline{\mathbf{u}}_1; \ \underline{\mathbf{u}}_1\right) \tag{19}$$

where  $\overline{\mathbf{u}}_1$  and  $\underline{\mathbf{u}}_1$  are the important and unimportant elements of  $\mathbf{u}_1$ , respectively. Therefore, we have

$$\beta_1 = \|\mathbf{u}_1\| = \|\overline{\mathbf{u}}_1; \ \underline{\mathbf{u}}_1\| = \sqrt{\|\overline{\mathbf{u}}_1\|^2 + \|\underline{\mathbf{u}}_1\|^2}$$
 (20)

We let  $\overline{\beta}_1$  and  $\underline{\beta}_1$  to be the FORM-reliability index of the important and unimportant portion of  $\mathbf{u}_1$ , respectively, which are denoted by

$$\overline{\beta}_1 = \|\overline{\mathbf{u}}_1\| \tag{21}$$

$$\beta_1 = \left\| \underline{\mathbf{u}}_1 \right\| \tag{22}$$

The overall FORM-reliability index is

$$\beta_1 = \sqrt{\overline{\beta}_1^2 + \underline{\beta}_1^2} \tag{23}$$

The final MPP elements of the unimportant variables will be different from  $\underline{\boldsymbol{u}}_1$ , but the difference will be insignificant because the contributions of the unimportant variables are relatively small. For this reason, we fix the unimportant variables  $\underline{\boldsymbol{U}}$  at  $\underline{\boldsymbol{u}}_1$ , but we will still consider their contributions indicated by their FORM-reliability index  $\underline{\beta}_1$  in the final stage of the reliability analysis. Then the limit-state function becomes a function of  $\overline{\boldsymbol{U}}$  with reduced dimension. The new function is given by

$$Y = G(\overline{\mathbf{U}}) = g(\overline{\mathbf{U}}; \mathbf{u}_1) \tag{24}$$

For brevity, we denote the limit-state function as  $G(\overline{\mathbf{U}})$ .

## 3.3 Reliability analysis in the reduced space

We next perform the reliability analysis in the reduced dimensional space ( $\overline{\mathbf{U}}$  space). Once the dimension is reduced, the reliability can be solved either by numerical methods (FORM, SORM, SOSPA, etc.) or surrogate methods (kriging, PCE, machine learning, etc.).

In this study, we use SOSPA for the demonstration. SOSPA is a second order numerical method and is used to obtain the probability of failure of  $G(\overline{\mathbf{U}})$ . The first step of SOSPA is to find the MPP of  $G(\overline{\mathbf{U}})$  which is  $\overline{\mathbf{u}}_G^*$  by Eq. (6). The magnitude of  $\overline{\mathbf{u}}_G^*$  or the FORM-reliability index is

$$\overline{\beta}_{G} = \left\| \overline{\mathbf{u}}_{G}^{*} \right\| \tag{25}$$

Once  $\overline{\mathbf{u}}_{G}^{*}$  is available, we approximate  $G(\overline{\mathbf{U}})$  at  $\overline{\mathbf{u}}_{G}^{*}$  by the second order Taylor expansion by Eq. (8) and have

$$G(\overline{\mathbf{U}}) \approx G(\overline{\mathbf{u}}_{G}^{*}) + \nabla G(\overline{\mathbf{u}}_{G}^{*})^{\mathrm{T}} (\overline{\mathbf{U}} - \overline{\mathbf{u}}_{G}^{*}) + \frac{1}{2} (\overline{\mathbf{U}} - \overline{\mathbf{u}}_{G}^{*})^{\mathrm{T}} H(\overline{\mathbf{u}}_{G}^{*}) (\overline{\mathbf{U}} - \overline{\mathbf{u}}_{G}^{*})$$
(26)

Then the CGF  $K_G(t)$  of  $G(\overline{\mathbf{U}})$  is derived analytically by Eq. (26). The detailed derivations can be found in [45]. The Saddlepoint  $t_S$  is obtained by solving  $K_G'(t) = 0$ . The probability of failure of  $G(\overline{\mathbf{U}})$  is calculated by Eq. (11), and the solution is denoted by  $\overline{p}_f$ . The reliability index from SOSPA then is given by

$$\overline{\beta}_{G,SPA} = \left| \Phi^{-1} \left( \overline{p}_f \right) \right| \tag{27}$$

If all the derivatives are evaluated by a finite difference method, the number of function evaluations with respect to the dimension of  $\bar{\mathbf{U}}$  is  $k(\bar{n}+1)+\frac{1}{2}\bar{n}(\bar{n}+1)$  where k is the number of iterations of the MPP search.

## 3.4 Final reliability analysis

The final step is to integrate the reliability results from Steps 1 and 2 so that the contributions of both important and unimportant variables are accommodated. Next, we derive the equation for the integration. We at first look at the case where we do not do any dimension reduction. Let the MPP obtained without any dimension reduction be  $\mathbf{u}^*$ , and it is partitioned into

$$\mathbf{u}^* = \left(\overline{\mathbf{u}}^*; \ \underline{\mathbf{u}}^*\right) \tag{28}$$

where  $\overline{\mathbf{u}}^*$  and  $\underline{\mathbf{u}}^*$  are the important and unimportant elements of the MPP  $\mathbf{u}^*$ . According to Eqs. (21), (22), and (23), we have  $\overline{\beta} = ||\overline{\mathbf{u}}^*||$ ,  $\beta = ||\underline{\mathbf{u}}^*||$ , and therefore

$$\beta = \sqrt{\|\overline{\mathbf{u}}^*\|^2 + \|\underline{\mathbf{u}}^*\|^2} = \sqrt{\overline{\beta}^2 + \underline{\beta}^2}$$
 (29)

We now look at the case with dimension reduction. As discussed in Step 1, we assume the MPP of unimportant variables to be the MPP from the first iteration; namely  $\underline{\mathbf{u}}^* = \mathbf{u}_1$ . Then

$$\beta \approx \left\| \underline{\mathbf{u}}_1 \right\| \tag{30}$$

In Step 2, we also perform the MPP search in the reduced space with unimportant variables fixed at  $\underline{\mathbf{u}}_1$ . This produces the MPP  $\overline{\mathbf{u}}_G^*$  and FORM-reliability index  $\overline{\beta}_G = \|\overline{\mathbf{u}}_G^*\|$ . Next, we prove that  $\overline{\mathbf{u}}_G^* = \overline{\mathbf{u}}^*$ , and therefore  $\overline{\beta} = \overline{\beta}_G$ . Then we can use Eq. (29) to integrate the results in Steps 1 and 2.

Because in the original space  $\mathbf{u}^*$  is found at the limit state  $g(T(\mathbf{U})) = 0$ , we have

$$g(T(\mathbf{u}^*)) = g(T(\overline{\mathbf{u}}^*; \mathbf{u}^*)) = 0$$
(31)

In the reduced space, for the same reason we have

$$G(\overline{\mathbf{u}}_{G}^{*}) = 0 \tag{32}$$

Assume that the MPPs of  $g(T(\overline{\mathbf{U}}; \underline{\mathbf{U}}))$  and  $G(\overline{\mathbf{U}})$  are unique, in other words,  $\mathbf{u}^* = (\overline{\mathbf{u}}^*; \mathbf{u}^*)$  and  $\overline{\mathbf{u}}_G^*$  are unique.

By substituting the MPP  $\mathbf{u}^*$  into Eqs. (15) and (17), we have

$$\mathbf{u}^* = -\beta \mathbf{\alpha} = -\beta \frac{\left(\frac{\partial g(T(\mathbf{u}^*))}{\partial u_i^*}\right)_{1,2,\dots,n}}{\|\nabla g(T(\mathbf{u}^*))\|}$$
(33)

Therefore, the important elements of the MPP can be expressed as

$$\overline{\mathbf{u}}^* = -\beta \overline{\mathbf{\alpha}} = -\beta \frac{\left(\frac{\partial g}{\partial \overline{U}_i}\right)_{1,\overline{n}}\Big|_{\mathbf{u}^*}}{\|\nabla g(T(\mathbf{u}^*))\|} = -\beta' \left(\frac{\partial g}{\partial \overline{U}_i}\right)_{1,\overline{n}}\Big|_{*}$$
(34)

$$\beta' = \frac{\beta}{\|\nabla g(T(\mathbf{u}^*))\|} \tag{35}$$

Now we relate  $\left(\frac{\partial g}{\partial \overline{U}_i}\right)_{1,\overline{n}}\Big|_{\mathbf{U}^*}$  with the reduced space.

$$\left. \left( \frac{\partial g}{\partial \overline{U}_{i}} \right)_{1,\overline{n}} \right|_{\mathbf{u}^{*}} = \left. \left( \frac{\partial g \left( T(\overline{\mathbf{U}}; \underline{\mathbf{u}}^{*}) \right)}{\partial \overline{U}_{i}} \right)_{1,\overline{n}} \right|_{\overline{\mathbf{u}}^{*}} \\
= \left. \left( \frac{\partial G}{\partial \overline{U}_{i}} \right)_{1,\overline{n}} \right|_{\overline{\mathbf{u}}^{*}} = \nabla G(\overline{\mathbf{u}}^{*}) \tag{36}$$

where  $\nabla G(\overline{\mathbf{u}}^*)$  is the gradient of  $G(\overline{\mathbf{U}})$  at  $\overline{\mathbf{u}}^*$ .

Then  $\overline{\mathbf{u}}^*$  is rewritten as

$$\overline{\mathbf{u}}^* = -\beta' \nabla G(\overline{\mathbf{u}}^*) \tag{37}$$

which indicates that  $\overline{\mathbf{u}}^*$  is perpendicular to  $G(\overline{\mathbf{U}}) = 0$ . Since  $g(\mathbf{u}^*) = g(\overline{\mathbf{u}}^*; \underline{\mathbf{u}}^*) = 0$ , we have  $G(\overline{\mathbf{u}}^*) = 0$ , which means that  $\overline{\mathbf{u}}^*$  is on the surface of  $G(\overline{\mathbf{U}}) = 0$  and is in the opposite direction of the gradient  $\nabla G(\overline{\mathbf{u}}^*)$ . Therefore,  $\overline{\mathbf{u}}^*$  is the shortest distance point from the original to the limit state surface  $G(\overline{\mathbf{u}}^*) = 0$  in the space of  $\overline{\mathbf{U}}$  and is the MPP of  $G(\overline{\mathbf{U}})$ ; namely

$$\overline{\mathbf{u}}^* = \overline{\mathbf{u}}_{\mathsf{G}}^* \tag{38}$$

Since  $\overline{\beta} = ||\overline{\mathbf{u}}^*||$ ,  $\overline{\beta}_G = ||\overline{\mathbf{u}}_G^*||$ , we have

$$\overline{\beta}_G = \overline{\beta} \tag{39}$$

Then Eq. (29) can be rewritten as

$$\beta = \sqrt{\overline{\beta}_G^2 + \underline{\beta}^2} \tag{40}$$

Because  $\underline{\mathbf{u}}_1 \leq c$ ,  $\underline{\beta} = \|\underline{\mathbf{u}}_1\|$  is far less than  $\overline{\beta}_G$ , namely,  $\underline{\beta} \ll \overline{\beta}_G$ , which means that  $\overline{\beta}_G$  dominates the accuracy of  $\beta$ . We now replace the FORM-reliability index  $\overline{\beta}_G$  with the more

accurate reliability index  $\overline{\beta}_{G,SPA}$  in Eq. (27), and then we obtain the final reliability index

$$\beta_{overall} = \sqrt{\overline{\beta}_{G,SPA}^2 + \underline{\beta}^2}$$
 (41)

Then the final probability of failure is obtained by

$$p_{f,overall} = \Phi(-\beta_{overall}) \tag{42}$$

## 3.5 Numerical procedure

The numerical procedure of the proposed dimension reduction method is summarized below.

- 1) Dimension reduction: Perform one step of the MPP search to obtain one-step MPP  $\mathbf{u}_1$ , identify the important and unimportant random variables by  $u_{1i} \leq c$ , and partition input variables as  $\mathbf{U} = (\overline{\mathbf{U}}; \underline{\mathbf{U}})$  and  $\mathbf{u}_1 = (\overline{\mathbf{u}}_1; \underline{\mathbf{u}}_1)$ , then calculated FORM-reliability index  $\underline{\beta} = \|\underline{\mathbf{u}}_1\|$ ; fix the unimportant variables  $\underline{\mathbf{U}}$  at  $\underline{\mathbf{u}}_1$  and obtain a new limit-state function  $G(\overline{\mathbf{U}}) = g(T(\overline{\mathbf{U}}; \underline{\mathbf{u}}_1))$  with reduced dimension.
- 2) Reliability analysis in  $\overline{\bf U}$  space: Use an accurate reliability method such as SOSPA to find the probability of failure  $\overline{p}_f$  based on  $G(\overline{\bf U})$  and calculate the corresponding reliability index, which is  $\overline{\beta}_{G,SPA}$  if SOSPA is used.
- 3) Final reliability analysis: Calculate the final reliability index by  $\beta_{overall} = \sqrt{\overline{\beta}_{G,SPA}^2 + \underline{\beta}^2}$  and the final probability of failure by  $p_{f,overall} = \Phi(-\beta_{overall})$ .

## 4. Examples

In this section, we use three examples to demonstrate the proposed method. Example 1 is a mathematical problem with all the input variables normally distributed. It is presented step by step to show all the details of the proposed method so that an interested reader can easily repeat the process and reproduce the result. Example 2 involves a cantilever beam with over 200 random variables, some of which follow non-normal distributions. Example 3 shows a truss system with 52 bars and 110 random variables, some of which follow extreme value distributions, and the limit-state function is a black-box function.

For comparison, we use MCS, FORM, SOSPA, and DR-SOSPA for all examples. MCS, FORM, and SOSPA are performed without dimension reduction. DR-SOSPA is the proposed method that employs SOSPA in the reduced dimensional space and accounts for the effects of eliminated variables. To evaluate the advantage of accounting for the effects of eliminated variables, we also compare DR-SOSPA with the method that employs SOSPA in the reduced dimensional space, but the eliminated variables are fixed at their means. We denoted the latter method DR-SOSPA-M. The result of MCS is served as a reference for the accuracy comparison, and the relative error of a non-MCS method with respect to MCS is defined by

$$\varepsilon = \left| \frac{p_f - p_{f,MCS}}{p_{f,MCS}} \right| \times 100\% \tag{43}$$

where  $p_f$  and  $p_{f,MCS}$  are the probabilities of failure obtained by a non-MCS and MCS, respectively. The number of function calls (FC) and the coefficient of efficiency (CoE) are used to measure the efficiency. The latter is defined by

$$CoE = \frac{The number of function calls}{The number of random variables}$$
 (44)

## 4.1 Example 1: a mathematical problem

The testing problem is a parabolic function given by

$$g(\mathbf{U}) = 20 - 3\sum_{i=1}^{5} U_i(1 + 0.1U_i) - \sum_{i=6}^{100} k_i U_i$$
 (45)

where  $U_i$ , i = 1,2,...,100 are all independent standard normal random variables, namely  $U_i \sim N(0,1^2)$ , and  $k_i$  is the coefficient of a linear term,  $k_i = 0.08$  for i = 6,7,...,100.

Following the procedure in Sec. 3.5, we first perform FOSM to obtain the first-iteration MPP  $\mathbf{u_1}$ . By setting a small quantity c=0.1 and using  $u_{1i} \leq c$  to identify important variables, we find that five variables are important, and they are  $\overline{\mathbf{U}} = (U_1, U_2, U_3, U_4, U_5)^{\mathrm{T}}$ . The unimportant variables are  $\underline{\mathbf{U}} = (U_6, U_7, ..., U_{100})^{\mathrm{T}}$ . Then  $\mathbf{u_1}$  is partitioned into  $(\overline{\mathbf{u}_1}; \underline{\mathbf{u}_1})$ , accordingly. The reliability index of unimportant variables is given by  $\underline{\beta} = \|\underline{\mathbf{u}_1}\| = 0.3419$ . It represents the contribution of the unimportant variables to the reliability. Then, we fix  $\underline{\mathbf{U}}$  at the  $\underline{\mathbf{u}_1}$  and have

$$g(\mathbf{U}) \approx G(\overline{\mathbf{U}}) = 20 - 3\sum_{i=1}^{5} U_i(1 + 0.1U_i) - \sum_{i=6}^{100} k_j \underline{u}_{1j}$$
 (46)

Thus, the dimension is reduced to 5 from 100.

Next, we conduct reliability analysis in  $\overline{\bf U}$  space. We first perform the MPP search for  $G(\overline{\bf U})$ , which results in the MPP  $\overline{\bf u}_{\bf g}^*=(1.1770,1.1770,1.1770,1.1770,1.1770)^{\rm T}$ . We then calculate the Hessian matrix of  $G(\overline{\bf U})$  at  $\overline{\bf u}_{\bf g}^*$  and use SOSPA, which results in the probability of failure  $\overline{p}_f=6.7352\times 10^{-3}$ . Then the reliability index of the important variables is obtained by  $\overline{\beta}_{G,SPA}=2.4711$ . The total reliability index, which accommodates both important and unimportant variables, is calculated by  $\beta_{overall}=\sqrt{\overline{\beta}_{G,SPA}^2+\underline{\beta}^2}=2.4946$ . The final probability of failure is given by  $p_{f,overall}=\Phi(-\beta_{overall})=6.3044\times 10^{-3}$ . The results of all the methods are summarized in Table 1.

The results in Table 1 show that SOSPA, DR-SOSPA, and DR-SOSPA-M accurately predict the probability of failure. Compared with the results of SOSPA with 5,555 function calls and an error of 0.16%, the proposed method needs 146 function calls and CoE = 1.46, only increasing the error to 0.59%. Although DR-SOSPA-M maintains the same efficiency as the

proposed method, the accuracy of DR-SOSPA-M is worse than DR-SOSPA because it ignores the joint influence of the unimportant variables. FORM do not produce an accurate result.

**Table 1** Probability of failure of Example 1

Methods	$p_f$	Error	FC	СоЕ
	,	(%)		
MCS	$6.3416 \times 10^{-3}$	-	1e7	$10^{5}$
FORM	$3.9966 \times 10^{-5}$	36.98	404	4.04
SOSPA	$6.3515 \times 10^{-3}$	0.16	5,555	55.55
DR-SOSPA-M	$6.1501 \times 10^{-3}$	3.02	146	1.46
DR-SOSPA	$6.3044 \times 10^{-3}$	0.59	146	1.46

## 4.2 Example 2: a cantilever beam

A cantilever is shown in Fig. 2. It is subjected to 106 random forces on the top surface, in which six of them  $(F_i, i = 1, 2, ..., 6)$  are lognormally distributed, and the rest  $(F_i, i = 7, 8, ..., 106)$  follow normal distributions. The locations of the forces are

random variables that are normally distributed, which are denoted by  $l_{F_i}$ , i = 1,2,...,106. The width w, height h, and the yield strength  $S_y$  are normally distributed. All the random variables are independent. The distributions are shown in Table 2.

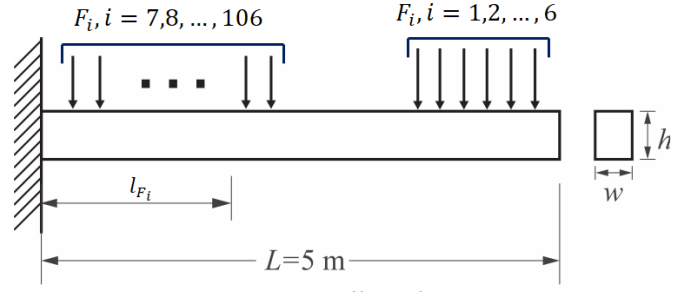


Fig. 2 A cantilever beam

**Table 2** Distributions of random variables in Example 2

Distribution	Mean	Standard deviation
Normal	720	60
Normal	0.2	0.001
Normal	0.4	0.001
Lognormal	30 + 5i	2.4 + 0.4i
Normal	4.3 + 0.1i	0.01
Normal	10	1
Normal	0.02i	0.01
	Normal Normal Normal Lognormal Normal Normal	Normal       720         Normal       0.2         Normal       0.4         Lognormal       30 + 5i         Normal       4.3 + 0.1i         Normal       10

The serviceability state depends on the stress at root of the beam. The maximal stress should not exceed the yield strength, and then the limit-state function is given by

$$g(\mathbf{X}) = S_y - \frac{6\sum_{i=1}^{106} F_i l_{F_i}}{wh^2}$$
 (47)

We first perform FOSM to obtain the first-step MPP  $\mathbf{u_1}$ . Using c=0.01, we obtain nine important variables  $\overline{\mathbf{U}}=(S_y,w,h,F_1,F_2,\ldots,F_6)^{\mathrm{T}}$  and the reliability index of unimportant variables  $\underline{\beta}=0.1666$ . Then we conduct reliability analysis in

 $\overline{\mathbf{U}}$  space using SOSPA and obtain  $\overline{p}_f=1.9481\times 10^{-6}$  and the corresponding reliability index is  $\overline{\beta}_{G,SPA}=4.6168$ . The total reliability index, which accommodates both important and unimportant variables, is calculated by  $\beta_{overall}=\sqrt{\overline{\beta}_{G,SPA}^2+\underline{\beta}^2}=4.6199$ . The probability of failure for the original limit state function is given by  $p_{f,overall}=\Phi(-\beta_{overall})=1.9201\times 10^{-6}$ . The results are summarized in Table 3.

Table 3 Probabilities of failure of Example 2

Methods	$p_f$	Error (%)	FC	CoE
MCS	$1.9106 \times 10^{-6}$	=	$1.6 \times 10^{9}$	$7.4 \times 10^{6}$
FORM	$1.7964 \times 10^{-6}$	5.9	648	3.0
SOSPA	$1.9200 \times 10^{-6}$	0.5	24,084	112.0
DR-SOSPA-M	$1.8926 \times 10^{-6}$	1.0	301	1.4
DR-SOSPA	$1.9201 \times 10^{-6}$	0.5	301	1.4

As the results indicate, FORM is the least accurate although it is efficient. The most accurate method is SOSPA with an error of 0.5%, but its efficiency is the worst with 24,084 function calls and CoE = 112. DR-SOSPA outperforms other methods with a slightly less accuracy (1.0%) compared with SOSPA and the highest efficiency (FC = 301 and CoE = 1.4).

## 4.3 Example 3: a truss system

This example is modified from [50]. The dome truss system is consisted of 52 bars with 21 nodes, as shown in Fig. 3. This is truss structure is similar to the roof of a stadium that consists of steel bars. To distinguish the difference between nodes and bars, the numbers with a dot mean nodes and the numbers without dot

denote bars. All the nodes lie on the imaginary hemisphere with a radius of 240 in. The young's moduli and the cross-sectional areas of bars follow normal distributions. The structure is subjected to six random forces at nodes 1-13, where  $F_1$  is applied to node 1,  $F_2$  is applied to nodes 2 and 4,  $F_3$  is applied to nodes 3 and 5,  $F_4$  is applied to nodes 6 and 10,  $F_5$  is applied to nodes 8 and 12, and  $F_6$  is applied to nodes 7, 9, 11, and 13. The directions of all the forces point to the center of the imaginary hemisphere. All the random variables are independent and are shown in Table 4. The limit-state function is given in Eq. (48) and is solved by the finite element method (FEM).

$$Y = \delta_0 - g(\mathbf{E}; \mathbf{A}; \mathbf{F}) \tag{48}$$

where  $\delta_0$  is the threshold displacement of node 1. A failure occurs when the displacement of node 1 exceeds  $\delta_0 = 0.7$  in.  $\mathbf{E} = [E_1, E_2, ..., E_{52}]^\mathrm{T}$  and  $\mathbf{A} = [A_1, A_2, ..., A_{52}]^\mathrm{T}$  are vectors of the young's modulus and cross-sectional areas, respectively.  $\mathbf{F} = [F_1, F_2, ..., F_6]^\mathrm{T}$  is the vector of the loads. The results are summarized in Table 5. FORM produces a

The results are summarized in Table 5. FORM produces a large error. SOSPA produces the most accurate result, but its efficiency is poor as it needs 6,771 function calls with CoE = 61.55. The error of DR-SOSPA is 3.38%, which is smaller than

the error of DR-SOSPA-M and is larger than SOSPA, and the computational burden is relieved significantly with only 179 function calls and CoE = 1.63.

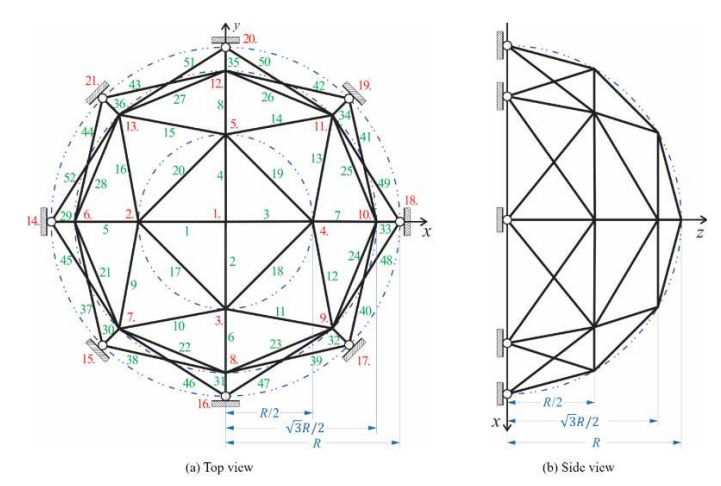


Fig. 3 A 52-bars truss system

**Table 4** Distributions of random variables in Example 3

Tuble 1 Distributions of fundom variables in Example 5				
Random variables	Distribution	Mean	Standard deviation	
$E_i, i = 1 \sim 50 \text{ (ksi)}$	Normal	$2.5 \times 10^{4}$	1000	
$A_i$ , $i = 1 \sim 8$ , and $29 \sim 36$ (in <sup>2</sup> )	Normal	2	0.001	
$A_i, i = 9 \sim 16 \text{ (in}^2)$	Normal	1.2	0.0006	
$A_i$ , $i = 17 \sim 28$ , and $37 \sim 52$ (in <sup>2</sup> )	Normal	0.6	0.0003	
$F_1$ (kip)	Normal	45	3.6	
$F_2$ (kip)	Extreme	40	6.0	
$F_3$ (kip)	Extreme	35	5.25	
$F_4$ (kip)	Normal	30	4.5	
$F_5$ (kip)	Normal	25	3.75	
$F_6$ (kip)	Normal	20	3	

Table 5 Estimates of probability of failure by different methods

Methods	$p_f$	Error (%)	FCs	CoE	
MCS	$5.10 \times 10^{-3}$	-	10 <sup>7</sup>	$9.09 \times 10^4$	
FORM	$5.7658 \times 10^{-3}$	13.05	444	5.05	
SOSPA	$5.0463 \times 10^{-3}$	1.05	6,660	61.55	
DR-SOSPA-M	$4.8532 \times 10^{-3}$	4.84	179	1.63	
DR-SOSPA	$4.9274 \times 10^{-3}$	3.38	179	1.63	

The univariate dimension reduction method [24] is another efficient method for high dimension problems. Since one univariate function usually needs at least 3 function evaluations, for an n-dimension problem, the least function call theoretically is 3n+1, which means the CoE for the univariate dimension reduction method is at least 3. The results of the above three examples show that the proposed method is more efficient than the univariate dimension reduction method. Therefore, we do not compare the proposed method with the univariate dimension reduction method since we already have the theoretical results for those three examples.

#### 5. Conclusion

The proposed method partitions the input random variables into two parts, important and unimportant variables. This is achieved by using the information from the first iteration of the First Order Reliability Method (FORM). With the unimportant random variables fixed at their percentile values obtained from FORM, the dimension is reduced to the number of important input random variables. Then the probability of failure is found by an accurate reliability method in the reduced space. The final probability of failure is obtained by integrating the probability of failure in the reduced space and the contributions of unimportant

variables. Hence, the dimension is reduced, and the contributions of all input variables are also accommodated, resulting in high accuracy and efficiency.

The proposed method works better if fewer important input variables are important. It cannot effectively reduce the dimension, however, when all input variables are important. If no dimension is reduced, the proposed dimension reduction strategy will not affect the performance of the method used in the second step (the high accurate reliability method in the reduced space in Sec. 3.5). In this case, one may use other dimension reduction methods that can reduce the dimension of the linear combinations of the original input variables. Our future work will improve the proposed method for the case where most of the input variables are important.

## Acknowledgements

We would like to acknowledge the support from the National Science Foundation under Grant No 1923799.

#### References

- [1] Hasofer, A. M., and Lind, N. C., 1974, "Exact and Invariant Second-Moment Code Format," Journal of the Engineering Mechanics division, 100(1), pp. 111-121.
- [2] Breitung, K., 1984, "Asymptotic Approximations for Multinormal Integrals," Journal of Engineering Mechanics, 110(3), pp. 357-366.
- [3] Hohenbichler, M., Gollwitzer, S., Kruse, W., and Rackwitz, R., 1987, "New Light on First-and Second-Order Reliability Methods," Structural Safety, 4(4), pp. 267-284.
- [4] Du, X., 2007, "Saddlepoint Approximation for Sequential Optimization and Reliability Analysis," Journal of Mechanical Design, 130(1).
- [5] Papadimitriou, D. I., Mourelatos, Z. P., and Hu, Z., 2018, "Reliability Analysis Using Second-Order Saddlepoint Approximation and Mixture Distributions," Journal of Mechanical Design, 141(2).
- [6] Jin, R., Du, X., and Chen, W., 2003, "The Use of Metamodeling Techniques for Optimization under Uncertainty," Structural and Multidisciplinary Optimization, 25(2), pp. 99-116.
- [7] Isukapalli, S., Roy, A., and Georgopoulos, P., 1998, "Stochastic Response Surface Methods (Srsms) for Uncertainty Propagation: Application to Environmental and Biological Systems," Risk Analysis, 18(3), pp. 351-363.
- [8] Hu, Z., and Du, X., 2015, "Mixed Efficient Global Optimization for Time-Dependent Reliability Analysis," Journal of Mechanical Design, 137(5).
- [9] Wu, H., Zhu, Z., and Du, X., 2020, "System Reliability Analysis with Autocorrelated Kriging Predictions," Journal of Mechanical Design, 142(10).
- [10] Echard, B., Gayton, N., and Lemaire, M., 2011, "AK-MCS: An Active Learning Reliability Method Combining Kriging and Monte Carlo Simulation," Structural Safety, 33(2), pp. 145-154.

- [11] Xi, Z., 2019, "Model-Based Reliability Analysis with Both Model Uncertainty and Parameter Uncertainty," Journal of Mechanical Design, 141(5).
- [12] Zhu, Z., and Du, X., 2016, "Reliability Analysis with Monte Carlo Simulation and Dependent Kriging Predictions," Journal of Mechanical Design, 138(12).
- [13] Zou, T., Mourelatos, Z. P., Mahadevan, S., and Tu, J., 2008, "An Indicator Response Surface Method for Simulation-Based Reliability Analysis," Journal of Mechanical Design, 130(7).
- [14] Papadrakakis, M., and Lagaros, N. D., 2002, "Reliability-Based Structural Optimization Using Neural Networks and Monte Carlo Simulation," Computer methods in Applied Mechanics and Engineering, 191(32), pp. 3491-3507.
- [15] Moarefzadeh, M., and Melchers, R., 1999, "Directional Importance Sampling for Ill-Proportioned Spaces," Structural Safety, 21(1), pp. 1-22.
- [16] Dey, A., and Mahadevan, S., 1998, "Ductile Structural System Reliability Analysis Using Adaptive Importance Sampling," Structural Safety, 20(2), pp. 137-154.
- [17] Rubinstein, R. Y., and Kroese, D. P., 2016, Simulation and the Monte Carlo Method, John Wiley & Sons.
- [18] Engelund, S., and Rackwitz, R., 1993, "A Benchmark Study on Importance Sampling Techniques in Structural Reliability," Structural Safety, 12(4), pp. 255-276.
- [19] Chen, W., Fuge, M., and Chazan, J., 2017, "Design Manifolds Capture the Intrinsic Complexity and Dimension of Design Spaces," Journal of Mechanical Design, 139(5).
- [20] Sarkar, S., Mondal, S., Joly, M., Lynch, M. E., Bopardikar, S. D., Acharya, R., and Perdikaris, P., 2019, "Multifidelity and Multiscale Bayesian Framework for High-Dimensional Engineering Design and Calibration," Journal of Mechanical Design, 141(12).
- [21] Pandita, P., Bilionis, I., and Panchal, J., 2016, "Extending Expected Improvement for High-Dimensional Stochastic Optimization of Expensive Black-Box Functions," Journal of Mechanical Design, 138(11).
- [22] Knerr, N., and Selva, D., 2016, "Cityplot: Visualization of High-Dimensional Design Spaces with Multiple Criteria," Journal of Mechanical Design, 138(9).
- [23] Ha, T. H., Lee, K., and Hwang, J. T., 2020, "Large-Scale Multidisciplinary Optimization under Uncertainty for Electric Vertical Takeoff and Landing Aircraft," Proc. AIAA Scitech 2020 Forum, p. 0904.
- [24] Rahman, S., and Xu, H., 2004, "A Univariate Dimension-Reduction Method for Multi-Dimensional Integration in Stochastic Mechanics," Probabilistic Engineering Mechanics, 19(4), pp. 393-408.
- [25] Rahman, S., 2011, "Global Sensitivity Analysis by Polynomial Dimensional Decomposition," Reliability Engineering & System Safety, 96(7), pp. 825-837.
- [26] Xie, S., Pan, B., and Du, X., 2017, "High Dimensional Model Representation for Hybrid Reliability Analysis with Dependent Interval Variables Constrained within Ellipsoids," Structural and Multidisciplinary Optimization, 56(6), pp. 1493-1505.

- [27] Hajikolaei, K. H., and Gary Wang, G., 2013, "High Dimensional Model Representation with Principal Component Analysis," Journal of Mechanical Design, 136(1).
- [28] Li, W., Lin, G., and Li, B., 2016, "Inverse Regression-Based Uncertainty Quantification Algorithms for High-Dimensional Models: Theory and Practice," Journal of Computational Physics, 321, pp. 259-278.
- [29] Pan, Q., and Dias, D., 2017, "Sliced Inverse Regression-Based Sparse Polynomial Chaos Expansions for Reliability Analysis in High Dimensions," Reliability Engineering & System Safety, 167, pp. 484-493.
- [30] Li, M., and Wang, Z., 2020, "Deep Learning for High-Dimensional Reliability Analysis," Mechanical Systems and Signal Processing, 139, p. 106399.
- [31] Tripathy, R., and Bilionis, I., 2019, "Deep Active Subspaces: A Scalable Method for High-Dimensional Uncertainty Propagation," Proc. International Design Engineering Technical Conferences and Computers and Information in Engineering Conference, American Society of Mechanical Engineers.
- [32] Zhou, T., and Peng, Y., 2020, "Structural Reliability Analysis Via Dimension Reduction, Adaptive Sampling, and Monte Carlo Simulation," Structural and Multidisciplinary Optimization, pp. 1-23.
- [33] Xu, J., and Wang, D., 2019, "Structural Reliability Analysis Based on Polynomial Chaos, Voronoi Cells and Dimension Reduction Technique," Reliability Engineering & System Safety, 185, pp. 329-340.
- [34] Sadoughi, M. K., Li, M., Hu, C., MacKenzie, C. A., Lee, S., and Eshghi, A. T., 2018, "A High-Dimensional Reliability Analysis Method for Simulation-Based Design under Uncertainty," Journal of Mechanical Design, 140(7).
- [35] Li, M., Sadoughi, M., Hu, C., Hu, Z., Eshghi, A. T., and Lee, S., 2019, "High-Dimensional Reliability-Based Design Optimization Involving Highly Nonlinear Constraints and Computationally Expensive Simulations," Journal of Mechanical Design, 141(5).
- [36] Li, K.-C., 1991, "Sliced Inverse Regression for Dimension Reduction," Journal of the American Statistical Association, 86(414), pp. 316-327.
- [37] Condra, L., 2001, Reliability Improvement with Design of Experiment, CRC Press.
- [38] Tripathy, R., Bilionis, I., and Gonzalez, M., 2016, "Gaussian Processes with Built-in Dimensionality Reduction: Applications to High-Dimensional Uncertainty Propagation," Journal of Computational Physics, 321, pp. 191-223.
- [39] Jiang, P., Missoum, S., and Chen, Z., 2014, "Optimal Svm Parameter Selection for Non-Separable and Unbalanced Datasets," Structural and Multidisciplinary Optimization, 50(4), pp. 523-535.
- [40] Dunteman, G. H., 1989, Principal Components Analysis, SAGE Publications, Inc.

- [41] Cook, R. D., 2018, "Principal Components, Sufficient Dimension Reduction, and Envelopes," Annual Review of Statistics and Its Application, 5(1), pp. 533-559
- [42] Bryant, F. B., and Yarnold, P. R., 1995, "Principal-Components Analysis and Exploratory and Confirmatory Factor Analysis," In L. G. Grimm & P. R. Yarnold (Eds.), Reading and understanding multivariate statistics (p. 99–136). American Psychological Association.
- [43] Lambe, A. B., and Martins, J. R., 2016, "Matrix-Free Aerostructural Optimization of Aircraft Wings," Structural and Multidisciplinary Optimization, 53(3), pp. 589-603.
- [44] Yu, X., and Du, X., 2006, "Reliability-Based Multidisciplinary Optimization for Aircraft Wing Design," Structures and Infrastructure Engineering, 2(3-4), pp. 277-289.
- [45] Hu, Z., and Du, X., 2018, "Saddlepoint Approximation Reliability Method for Quadratic Functions in Normal Variables," Structural Safety, 71, pp. 24-32.
- [46] Du, X., and Sudjianto, A., 2004, "First Order Saddlepoint Approximation for Reliability Analysis," AIAA Journal, 42(6), pp. 1199-1207.
- [47] Daniels, H. E., 1954, "Saddlepoint Approximations in Statistics," The Annals of Mathematical Statistics, pp. 631-650.
- [48] Lugannani, R., and Rice, S., 1980, "Saddle Point Approximation for the Distribution of the Sum of Independent Random Variables," Advances in Applied Probability, 12(2), pp. 475-490.
- [49] Du, X., and Chen, W., 2001, "A Most Probable Point-Based Method for Efficient Uncertainty Analysis," Journal of Design and Manufacturing automation, 4(1), pp. 47-66.
- [50] Zhang, Z., Jiang, C., Han, X., and Ruan, X., 2019, "A High-Precision Probabilistic Uncertainty Propagation Method for Problems Involving Multimodal Distributions," Mechanical Systems and Signal Processing, 126, pp. 21-41.